

Methane and environmental change during the Paleocene-Eocene thermal maximum (PETM): Modeling the PETM onset as a two-stage event

David A. Carozza,^{1,2} Lawrence A. Mysak,¹ and Gavin A. Schmidt³

Received 1 November 2010; revised 17 January 2011; accepted 26 January 2011; published 1 March 2011.

[1] An atmospheric CH₄ box model coupled to a global carbon cycle box model is used to constrain the carbon emission associated with the PETM and assess the role of CH₄ during this event. A range of atmospheric and oceanic emission scenarios representing different amounts, rates, and isotopic signatures of emitted carbon are used to model the PETM onset. The first 3 kyr of the onset, a pre-isotope excursion stage, is simulated by the atmospheric release of 900 to 1100 Pg C CH₄ with a $\delta^{13}\text{C}$ of -22 to -30% . For a global average warming of 3°C , a release of CO₂ to the ocean and CH₄ to the atmosphere totalling 900 to 1400 Pg C, with a $\delta^{13}\text{C}$ of -50 to -60% , simulates the subsequent 1-kyr isotope excursion stage. To explain the observations, the carbon must have been released over at most 500 years. The first stage results cannot be associated with any known PETM hypothesis. However, the second stage results are consistent with a methane hydrate source. More than a single source of carbon is required to explain the PETM onset. **Citation:** Carozza, D. A., L. A. Mysak, and G. A. Schmidt (2011), Methane and environmental change during the Paleocene-Eocene thermal maximum (PETM): Modeling the PETM onset as a two-stage event, *Geophys. Res. Lett.*, *38*, L05702, doi:10.1029/2010GL046038.

1. Introduction

[2] The Paleocene-Eocene thermal maximum (PETM), approximately 55.5 Myr ago, was characterized by a significant negative carbon isotope excursion (CIE) averaging approximately -3% , a regional surface warming ranging from 3 to 9°C , and a pronounced acidification of the Atlantic Ocean [Shuijs *et al.*, 2007a]. Based on these and other environmental changes, the PETM has been related to a tremendous release of CO₂ and/or CH₄ that was significantly depleted in ^{13}C [Dickens *et al.*, 1997], and thus its investigation can give important insight into the long-term future evolution of the carbon cycle.

[3] The PETM CIE has been related to a geologically rapid (<10 kyr) carbon release [Röhl *et al.*, 2000; Zachos *et al.*, 2007]; however, others have proposed a signifi-

cantly slower release (about 130 kyr) [Murphy *et al.*, 2010]. Prior to the light carbon injection, a brief (<10 kyr) period of oceanic [Thomas *et al.*, 2002; Sluijs *et al.*, 2007b] and continental [Secord *et al.*, 2010] warming, as well as dissolution of seafloor carbonates [Leon-Rodriguez and Dickens, 2010], is thought to have occurred, indicating that the carbon input that caused the CIE may not have produced the initial warming. Furthermore, CH₄ is thought to have played a pivotal role during the PETM because it is highly depleted in ^{13}C and is a strong greenhouse gas. Among hypotheses to explain the massive carbon input at the start of the PETM, the methane hydrate hypothesis [Dickens *et al.*, 1995] and the thermogenic CH₄ hypothesis [Svensen *et al.*, 2004] involve the release of CH₄ into the ocean and/or atmosphere.

[4] The cause and amount of the PETM carbon emission are still unresolved. Paleoclimate proxy results alone cannot be used to determine which hypothesis, or combination of hypotheses, best explain the PETM. Models are therefore useful to estimate the magnitude of the carbon emission and develop scenarios. In this study, the PETM is assumed to be associated with a rapid carbon input that caused the CIE, and the CIE is assumed to be preceded by a period of warming and carbonate dissolution. The PETM onset is thus modeled as a two-stage event using a global carbon cycle box model [Walker and Kasting, 1992, hereafter WK92] tuned to the pre-PETM period and coupled to an atmospheric CH₄ box model [Schmidt and Shindell, 2003, hereafter SS03]. Including the latter component allows us to assess the role of CH₄ during the PETM.

2. Model

[5] The WK92 box model simulates the first-order interactions and evolution of the global carbon cycle. Carbon-containing species are cycled through eight well-mixed reservoirs by means of parameterizations of physical, chemical, and biological processes. In contrast to earlier work, here the WK92 model is tuned to pre-PETM conditions and an error in the coding of five of the oceanic $\delta^{13}\text{C}$ equations is corrected (see auxiliary material).¹ In coupling the two-box CH₄ model of SS03 to WK92, atmospheric CH₄ interacts with the components of WK92 as it is oxidized into CO₂ and added to the atmospheric CO₂ reservoir. In response to the release of carbon to the ocean and/or atmosphere, the coupled model calculates the $\delta^{13}\text{C}$ of all reservoirs, the lysocline depth of each deep ocean reservoir,

¹Department of Atmospheric and Oceanic Sciences, McGill University, Montreal, Quebec, Canada.

²Now at Department of Earth and Planetary Sciences, McGill University, Montreal, Quebec, Canada.

³NASA Goddard Institute for Space Studies, New York, New York, USA.

and the concentrations of atmospheric CO₂, CH₄, and stratospheric water vapor.

3. Experimental Approach

[6] The PETM onset is proposed to consist of two stages. Stage 1, which occurs prior to the CIE, is composed of a notable warming and lysocline shoaling over 3 kyr [Thomas *et al.*, 2002; Sluijs *et al.*, 2007b; Secord *et al.*, 2010; Leon-Rodriguez and Dickens, 2010], whereas stage 2 comprises of an abrupt and large negative CIE, pronounced Atlantic lysocline shoaling, and further warming over 1 kyr [Röhl *et al.*, 2000; Zachos *et al.*, 2007] (Table S1).

[7] For each stage, atmospheric and oceanic emission scenarios that represent the range of plausible isotopic signatures, amounts, and rates of emitted CH₄ and CO₂ are simulated. Carbon dioxide is emitted into the atmosphere in one set of simulations (hereafter case 1) and into the Atlantic (hereafter case 2) in the other. Carbon is added to the Atlantic reservoir since this is the most likely location of an oceanic carbon release [Zeebe *et al.*, 2009]. Methane is emitted into the atmosphere, representing either a terrestrial CH₄ release or an oceanic CH₄ emission that has ascended through the water column and escaped unoxidized to the atmosphere.

[8] Seven isotopic signatures representing mantle carbon ($\delta^{13}\text{C} = -5\text{‰}$), organic CO₂ ($\delta^{13}\text{C} = -22\text{‰}$), thermogenic CH₄ ($\delta^{13}\text{C} = -35\text{‰}$), methane hydrate ($\delta^{13}\text{C} = -60\text{‰}$), and mixtures of these ($\delta^{13}\text{C} = -12, -30, -50\text{‰}$) are considered. In each stage, all combinations of CO₂ and CH₄ emissions totaling up to 5000 Pg C, using a resolution of 100 Pg C, are simulated. Carbon is released uniformly at the beginning of a stage for the duration of the emission, and five emission durations are examined for each stage (1: 50, 500, 1000, 2000, and 3000 years; 2: 50, 250, 500, 750, and 1000 years).

[9] Average lysocline shoaling and the global average CIE are calculated by the model. Based on the time-averaged increases in atmospheric CO₂, CH₄, and stratospheric water vapor calculated by the model, the anomalous forcing due to CO₂ and CH₄ is calculated from Forster *et al.* [2007] using baseline concentrations of 2280 [Winguth *et al.*, 2010] and 0.7 ppmv for CO₂ and CH₄, respectively; the anomalous forcing due to stratospheric water vapor is assumed to be $0.24 \text{ W m}^{-2} \text{ ppmv}^{-1}$ [Solomon *et al.*, 2010]. To determine the forcing necessary to reproduce the PETM temperature record and take climate sensitivity into consideration [Pagani *et al.*, 2006], the proxy-derived global average temperature increase ΔT is divided by the climate sensitivity parameter S' , the ratio of equilibrium temperature change to anomalous forcing as defined by Knutti and Hegerl [2008], which is thought to range from 0.5 to $1.0^\circ\text{C W}^{-1}\text{m}^2$ [Forster *et al.*, 2007]. For a range of ΔT (1 to 4 and 1 to 7°C for stages 1 and 2, respectively) and S' , the minimum total emission that is compatible with the CIE, Atlantic lysocline shoaling, and ΔT target characteristics (Table S1), is determined. Results within 15% of the target characteristics are assumed to be data-compatible.

[10] There is evidence of carbonate dissolution prior to the CIE [Leon-Rodriguez and Dickens, 2010]; however, it remains uncertain how much of the lysocline and calcite compensation depth shoaling occurred during stage 1. Here, it is assumed that a small shoaling of the Atlantic lysocline,

0.5 km, occurred during stage 1, with the remaining 1.5 km of shoaling occurring in stage 2. Similarly, a small CIE of 0.3‰ is assumed to have occurred during stage 1 [Thomas *et al.*, 2002; Sluijs *et al.*, 2007b], with a global excursion of -1.25‰ generated during stage 2 [Röhl *et al.*, 2000] (Table S1). Sensitivity analyses are performed to determine the impact on the results to changes in the assumptions.

4. Results

[11] Stage 1 target characteristics (Table S1) can be simulated by a total emission ranging from 900 to 1100 Pg C (Figure 1a) for case 1. This emission consists of 100 to 600 Pg C CO₂ (not shown) and 300 to 1100 Pg C CH₄ (Figure 1b). Methane dominates the total emission for ΔT larger than 1.5°C , whereas CO₂ plays a more important role for small ΔT and larger values of the climate sensitivity parameter S' . Only an emission duration of 50 years and a $\delta^{13}\text{C}$ signature of -22‰ are compatible with the characteristics of stage 1 (Figures 1c and 1d).

[12] For case 2, a total emission of 800 to 1100 Pg C (Figure 1e) is needed in order to be compatible with the characteristics of stage 1. In this case, the release of only 100 Pg C CO₂ (not shown) is required since larger oceanic emissions produce excessive amounts of lysocline shoaling, whereas an atmospheric release of 700 to 1100 Pg C CH₄ is required (Figure 1f). Emission durations of 50 and 500 years are compatible with stage 1 for the range of values of ΔT and S' (Figure 1g). As in case 1, only an isotopic $\delta^{13}\text{C}$ signature of -22‰ is compatible with the stage 1 target characteristics.

[13] Based on a stage 1 ΔT of 2°C [Thomas *et al.*, 2002], the results are generally robust with respect to the different emission locations of cases 1 and 2. Since the minimum total carbon emission (Figures 1a and 1e) and the CH₄ contribution (Figures 1b and 1f) are essentially the same in both cases for $\Delta T = 2^\circ\text{C}$, a purely CO₂ release is unable to explain the characteristics of stage 1. Hence, the emission of 900 to 1100 Pg C CH₄ to the atmosphere with a duration of 50 years and a $\delta^{13}\text{C}$ of -22‰ best simulates the proxy evidence of stage 1 (Figure 3).

[14] In case 1 of stage 2, no simulation is compatible with the characteristics. This arises because an atmospheric emission does not produce a large enough or an abrupt enough shoaling of the Atlantic lysocline. However, in case 2, a mixed emission of 900 to 3200 Pg C (Figure 2a) composed of 300 to 500 Pg C CO₂ to the ocean (not shown) and 400 to 2900 Pg C CH₄ (Figure 2b) to the atmosphere produces sufficient forcing, lysocline shoaling, and CIE to simulate stage 2. In particular, for $\Delta T = 3^\circ\text{C}$ [Winguth *et al.*, 2010], a mixed emission of 900 to 1400 Pg C consisting of 400 to 500 Pg C CO₂ to the ocean and 400 to 900 Pg C CH₄ to the atmosphere simulates stage 2. Durations of 50 and 250 years are data-compatible (Figure 2c); however, only a duration of 50 years is compatible with 3°C of warming. The $\delta^{13}\text{C}$ of emitted carbon ranges from -30 to -60‰ (Figure 2d), with $\delta^{13}\text{C}$ signatures of -50 and -60‰ being data-compatible for 3°C of warming. Therefore, the emission of 400 to 900 Pg C CH₄ to the atmosphere and 400 to 500 Pg C CO₂ to the ocean, with a duration of 50 years and $\delta^{13}\text{C}$ ranging from -50 to -60‰ , best simulates stage 2 (Figure 3).

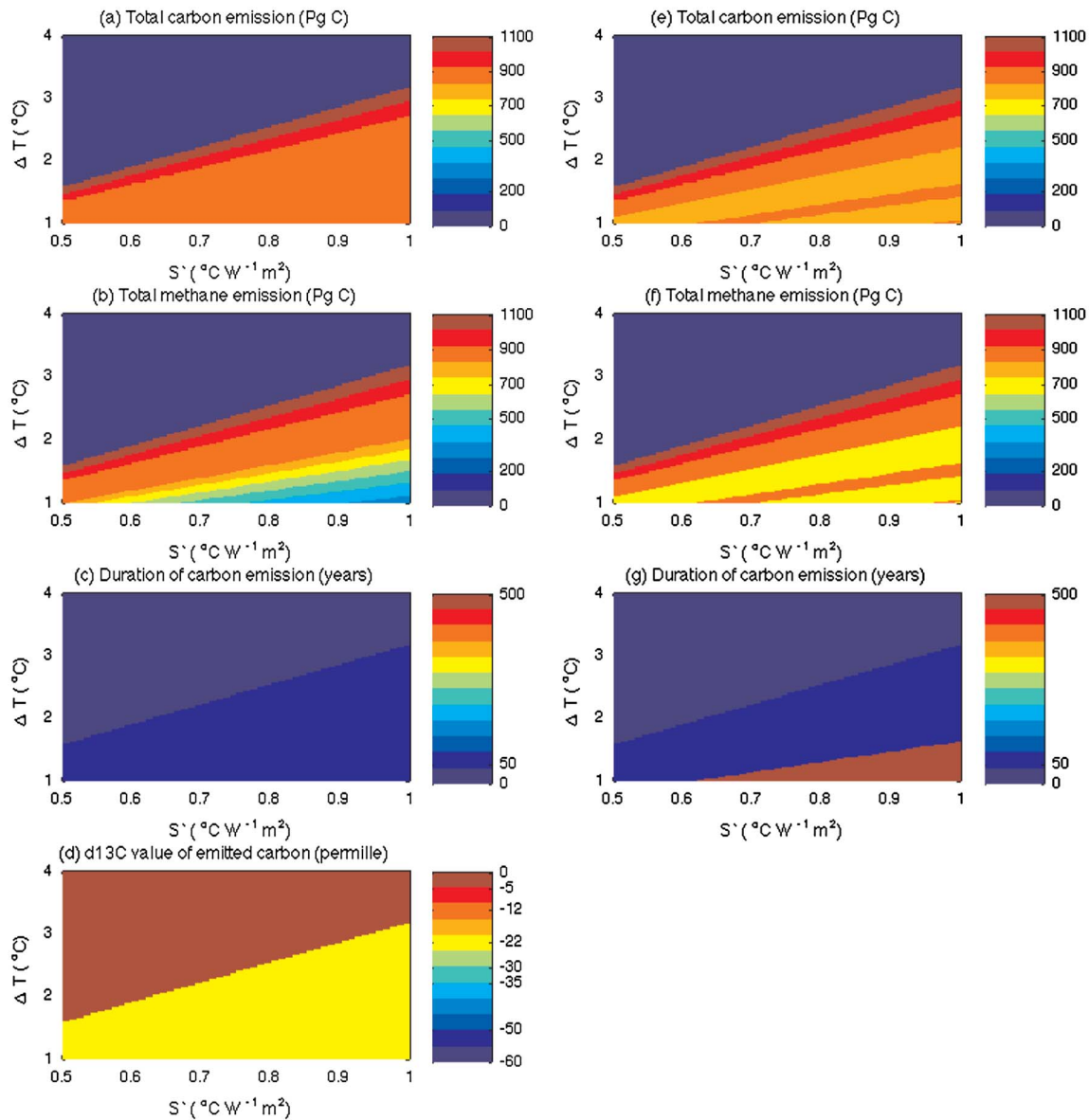


Figure 1. (a) Total carbon (CO_2 and CH_4) emission (Pg C), and (b) total methane emission (Pg C) required to reproduce the target characteristics (Table S1) for case 1 of stage 1, as a function of temperature change ΔT ($^{\circ}\text{C}$) and the climate sensitivity parameter S' ($^{\circ}\text{C W}^{-1}\text{m}^2$). (c) Emission duration (years) is plotted, and (d) isotopic $\delta^{13}\text{C}$ value of emitted carbon (‰) is represented. (e–g) Same as Figures 1a–1c, but for case 2 of stage 1. The plot of the isotopic signature for case 2 is the same as in Figure 1d. A value of zero indicates that no emission scenario is able to reproduce the observed characteristics.

[15] A variety of sensitivity tests have also been performed. The results are robust with respect to the assumptions of the baseline concentrations of CO_2 and CH_4 . The impact of alternative target characteristics (Table S1) is examined. In stage 1, for a low (high) Atlantic lysocline shoaling target, the minimum total emission decreases to 500 Pg C (increases to range from 1300 to 2000 Pg C), whereas the $\delta^{13}\text{C}$ value of the emitted carbon increases to -30‰ (does not change). A high CIE target increases the required $\delta^{13}\text{C}$ signature to -30‰ ; however, no simulation is data-compatible for the low CIE target. For all choices of the stage 1 targets, CH_4 remains the major constituent of the emission. Stage 2 results are not significantly affected by

changes in the target characteristics. Alternative CO_2 emission locations (Indian, Pacific, and thermocline reservoirs) have also been tested. Stage 1 results are not impacted by the choice of emission location, whereas for stage 2 there are no simulations consistent with the targets because the Atlantic lysocline shoals too little. Different stage 1 lengths (1, 5, and 10 kyr) have also been analyzed. For a stage 1 length of 1 kyr, CO_2 plays a more important role (Figure S1b) than in the 3-kyr case, whereas for a 5-kyr stage 1 length, data-compatible simulations only exist for low ΔT and high S' , and no simulations produce a ΔT of 2°C (Figure S2a). Using a 10-kyr stage 1 length, data-compatible simulations only exist for high Atlantic lysocline shoaling and CIE

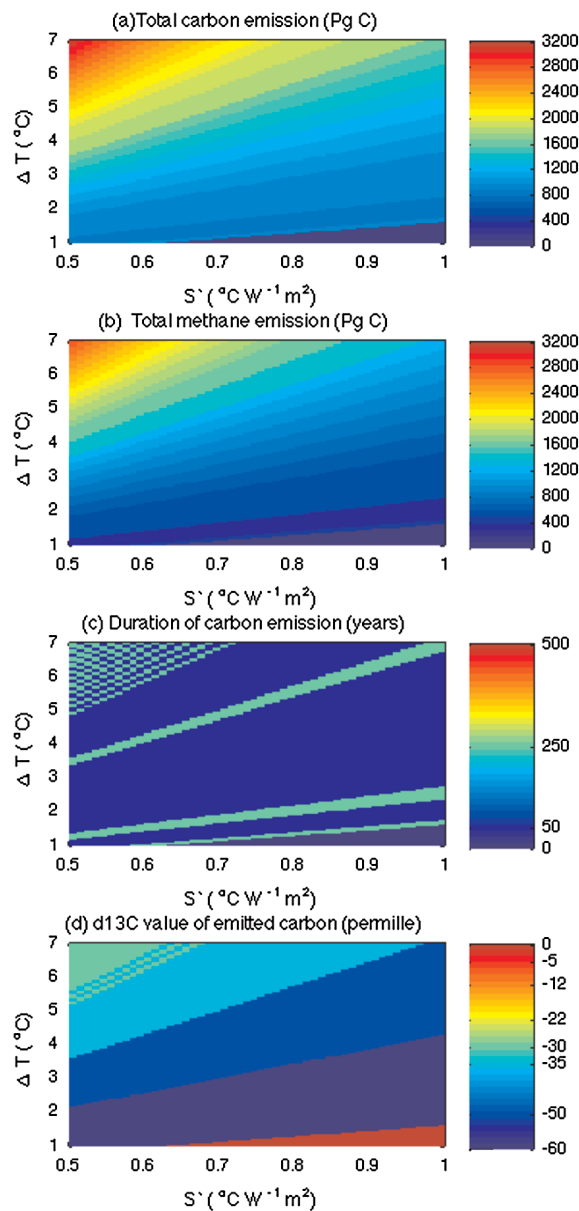


Figure 2. As in Figures 1a–1d, but for case 2 of stage 2.

targets; however, this is only the case for low ΔT and high S' (Figure S3a).

5. Discussion and Concluding Remarks

[16] The stage 1 simulation does not correspond to a known hypothesis for the PETM. A release of methane hydrate produces too large a CIE. Although a thermogenic CH_4 source has too slow a release, sensitivity tests indicate that this carbon source can be isotopically consistent with stage 1 targets. Organic carbon released to the atmosphere through the burning of terrestrial biomass [Kurtz *et al.*, 2003] is isotopically consistent with the results, and sensitivity tests show that CO_2 may have been an important contributor to forcing during stage 1; however, the modeled release is significantly quicker than that proposed. No emission of CO_2 alone is compatible with the characteristics

of stage 1. Sensitivity tests show that a 1-kyr stage 1 length is plausible, but that it is difficult to explain the characteristic targets using stage 1 lengths of 5 and 10 kyr.

[17] Stage 2 results are consistent with a release of methane hydrate, where oxidation of CH_4 takes place in both the ocean and the atmosphere. Oceanic oxidation of CH_4 is required to generate the abrupt shoaling of the Atlantic lysocline, while a concurrent emission of CH_4 to the atmosphere is required to reproduce the surface temperature change record. For 3°C of warming, 30 to 45% of the total carbon release is oxidized in the ocean, which is consistent with Zeebe *et al.* [2009]. Furthermore, the Pacific lysocline shoals by less than 0.1 km throughout stages 1 and 2 (Figure 3), and thus agrees with the large observed lysocline shoaling difference between the Atlantic and Pacific [Zeebe *et al.*, 2009]. For CH_4 to reproduce the characteristics of stage 2, however, it must be abruptly released. These results are therefore consistent with a catastrophic release of methane hydrate from sediment, followed by the oxidation of a part of this CH_4 in the water column and the escape of the remaining CH_4 to the atmosphere.

[18] This study highlights the importance of (1) considering the temporal structure of high-resolution geochemical records in constraining the source, total release, and rate of emission of carbon during the PETM and other hyperthermal climate events, and (2) recognizing uncertainty in paleocli-

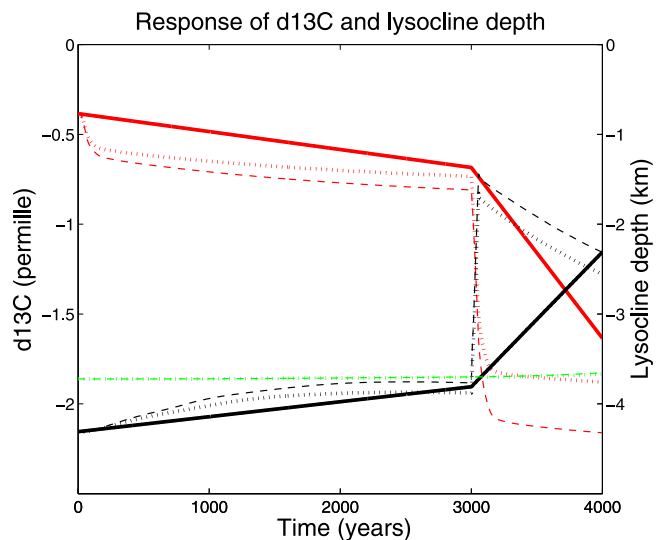


Figure 3. Response of global $\delta^{13}\text{C}$ (red curves), Atlantic lysocline depth (black curves), and Pacific lysocline depth (green curves) to carbon emissions during stages 1 and 2, of lengths 3 and 1 kyr, respectively. Solid curves represent observed changes of the two variables based on references cited assuming a piecewise linear structure. Dashed and dotted lines represent the simulated evolution of the two variables for a low and a high value of climate sensitivity parameter S' (0.65 and $0.85^{\circ}\text{C W}^{-1}\text{m}^2$). Assuming ΔT of 2 and 3°C for stages 1 and 2, respectively, the low value of S' corresponds to the emission of 1100 Pg C CH_4 in stage 1 (Figures 1b and 1f) and of 400 and 700 Pg C CO_2 and CH_4 , respectively, in stage 2 (Figures 2a and 2b). The high S' value corresponds to the emission of 900 Pg C CH_4 in stage 1 (Figures 1b and 1f) and of 400 and 500 Pg C CO_2 and CH_4 , respectively, in stage 2 (Figures 2a and 2b).

mate proxy and climate sensitivity estimates. By testing a range of values of ΔT and S' , the uncertainty in these two quantities is examined, and their impact on the features of the emission are quantified. Furthermore, by modeling the PETM onset as two separate stages, it is shown that at least two different carbon sources are required to simulate the PETM [Sluijs *et al.*, 2007b], and therefore that current hypotheses of the cause of the PETM may require revision.

[19] **Acknowledgments.** The authors are grateful to J.F. Kasting for providing the Walker-Kasting carbon cycle box model code and to two reviewers for their insightful comments. This work was supported by scholarships awarded to DAC from Hydro-Québec, NSERC, FQRNT, and the Birks Family Foundation. This work was also supported by an NSERC Discovery Grant awarded to LAM.

References

- Dickens, G. R., J. R. O'Neil, D. K. Rea, and R. M. Owen (1995), Dissociation of oceanic methane hydrate as a cause of the carbon isotope excursion at the end of the Paleocene, *Paleoceanography*, *10*, 965–971, doi:10.1029/95PA02087.
- Dickens, G. R., M. M. Castillo, and J. C. G. Walker (1997), A blast of gas in the latest Paleocene: Simulating first-order effects of massive dissociation of oceanic methane hydrate, *Geology*, *25*, 259–262, doi:10.1130/0091-7613(1997)025.
- Forster, P., et al. (2007), Changes in Atmospheric Constituents and in Radiative Forcing, in *Climate Change 2007: The Physical Science Basis. Contribution of Working Group I to the Fourth Assessment Report of the Intergovernmental Panel on Climate Change*, edited by S. Solomon et al., pp. 131–234, Cambridge Univ. Press, Cambridge, U. K.
- Knutti, R., and G. C. Hegerl (2008), The equilibrium sensitivity of the Earth's temperature to radiation changes, *Nat. Geosci.*, *1*, 735–743, doi:10.1038/ngeo337.
- Kurtz, A. C., L. R. Kump, M. A. Arthur, J. C. Zachos, and A. Paytan (2003), Early Cenozoic decoupling of the global carbon and sulfur cycles, *Paleoceanography*, *18*(4), 1090, doi:10.1029/2003PA000908.
- Leon-Rodriguez, L., and G. R. Dickens (2010), Constraints on ocean acidification associated with rapid and massive carbon injections: The early Paleogene record at ocean drilling program site 1215, equatorial Pacific Ocean, *Palaeogeogr. Palaeoclimatol. Palaeoecol.*, *298*(3–4), 409–420, doi:10.1016/j.palaeo.2010.10.029.
- Murphy, B. H., K. A. Farley, and J. C. Zachos (2010), An extraterrestrial ^3He -based timescale for the Paleocene-Eocene thermal maximum (PETM) from Walvis Ridge, IODP Site 1266, *Geochim. Cosmochim. Acta*, *74*, 5098–5108, doi:10.1016/j.gca.2010.03.039.
- Pagani, M., K. Caldeira, D. Archer, and J. C. Zachos (2006), Atmosphere: An ancient carbon mystery, *Science*, *314*(5805), 1556–1557, doi:10.1126/science.1136110.
- Röhl, U., T. J. Bralower, R. D. Norris, and G. Wefer (2000), New chronology for the late Paleocene thermal maximum and its environmental implications, *Geology*, *28*, 927–930, doi:10.1130/0091-7613(2000)28.
- Schmidt, G. A., and D. T. Shindell (2003), Atmospheric composition, radiative forcing, and climate change as a consequence of a massive methane release from gas hydrates, *Paleoceanography*, *18*(1), 1004, doi:10.1029/2002PA000757.
- Secord, R., P. D. Gingerich, K. C. Lohmann, and K. G. MacLeod (2010), Continental warming preceding the Palaeocene-Eocene thermal maximum, *Nature*, *467*, 955–958, doi:10.1038/nature09441.
- Sluijs, A., G. J. Bowen, L. J. Lourens, and E. Thomas (2007a), The Palaeocene-Eocene Thermal Maximum super greenhouse: biotic and geochemical signatures, age models and mechanisms of global change, in *Deep-Time Perspectives on Climate Change: Marrying the Signal from Computer Models and Biological Proxies*, edited by M. Williams et al., pp. 323–349, Geol. Soc., London.
- Sluijs, A., et al. (2007b), Environmental precursors to rapid light carbon injection at the Palaeocene/Eocene boundary, *Nature*, *450*, 1218–1221, doi:10.1038/nature06400.
- Solomon, S., K. H. Rosenlof, R. W. Portmann, J. S. Daniel, S. M. Davis, T. J. Sanford, and G. Plattner (2010), Contributions of stratospheric water vapor to decadal changes in the rate of global warming, *Science*, *327*, 1219–1223, doi:10.1126/science.1182488.
- Svensen, H., S. Planke, A. Malthes-Sørensen, B. Jamtveit, R. Myklebust, T. Rasmussen Eidem, and S. S. Rey (2004), Release of methane from a volcanic basin as a mechanism for initial Eocene global warming, *Nature*, *429*, 542–545, doi:10.1038/nature02566.
- Thomas, D. J., J. C. Zachos, T. J. Bralower, E. Thomas, and S. Bohaty (2002), Warming the fuel for the fire: Evidence for the thermal dissociation of methane hydrate during the Paleocene-Eocene thermal maximum, *Geology*, *30*, 1067–1070, doi:10.1130/0091-7613(2002)030<1067:WTFITF>2.0.CO;2.
- Walker, J. C., and J. F. Kasting (1992), Effects of fuel and forest conservation on future levels of atmospheric carbon dioxide, *Palaeogeogr. Palaeoclimatol. Palaeoecol.*, *97*, 151–189.
- Winguth, A., C. Shellito, C. Shields, and C. Winguth (2010), Climate response at the Paleocene-Eocene thermal maximum to greenhouse gas forcing—A model study with CCSM3, *J. Clim.*, *23*(10), 2562–2584, doi:10.1175/2009JCLI3113.1.
- Zachos, J. C., S. M. Bohaty, C. M. John, H. McCarren, D. C. Kelly, and T. Nielsen (2007), The Palaeocene-Eocene carbon isotope excursion: Constraints from individual shell planktonic foraminifer records, *Philos. Trans. R. Soc. A*, *365*, 1829–1842, doi:10.1098/rsta.2007.2045.
- Zeebe, R. E., J. C. Zachos, and G. R. Dickens (2009), Carbon dioxide forcing alone insufficient to explain Palaeocene-Eocene thermal maximum warming, *Nature Geosci.*, *2*, 576–580, doi:10.1038/ngeo578.

D. A. Carozza, Department of Earth and Planetary Sciences, McGill University, 3450 University St., Montreal, QT H3A 2A7, Canada. (david.carozza@mcgill.ca)

L. A. Mysak, Department of Atmospheric and Oceanic Sciences, McGill University, 805 Sherbrooke St. West, Montreal, QT H3A 2K6, Canada.

G. A. Schmidt, NASA Goddard Institute for Space Studies, 2880 Broadway, New York, NY 10025, USA.